Journal of Power Sources 342 (2017) 598–604

Contents lists available at ScienceDirect

Journal of Power Sources

journal homepage: www.elsevier.com/locate/jpowsour

Innovative heating of large-size automotive Li-ion cells

Xiao-Guang Yang, Teng Liu, Chao-Yang Wang*

Department of Mechanical and Nuclear Engineering and Electrochemical Engine Center (ECEC), The Pennsylvania State University, University Park, PA 16802, USA

HIGHLIGHTS

- Speed of conventional heating methods is too slow for large-size Li-ion cells.
- Power of external heating is limited by risk of localized overheating.
- Self-heating Li-ion battery can achieve rapid, uniform and energy-efficient heating.

GRAPHICAL ABSTRACT

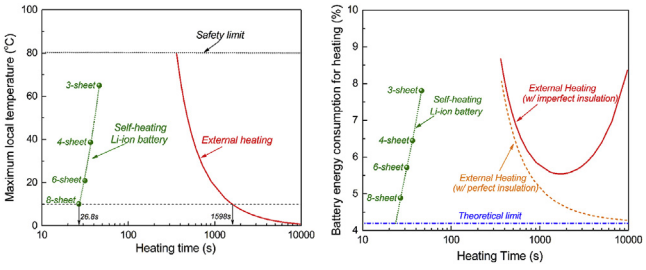

ARTICLE INFO

Article history:
Received 23 November 2016
Received in revised form
7 December 2016
Accepted 25 December 2016

Keywords:
Li-ion cell
Automotive
Heating
Low temperatures

ABSTRACT

Automotive Li-ion cells are becoming much larger and thicker in order to reduce the cell count and increase battery reliability, posing a new challenge to battery heating from the cold ambient due to poor through-plane heat transfer across a cell's multiple layers of electrodes and separators. In this work, widely used heating methods, including internal heating using the cell's resistance and external heating by resistive heaters, are compared with the recently developed self-heating Li-ion battery (SHLB) with special attention to the heating speed and maximum local temperature critical to battery safety. Both conventional methods are found to be slow due to low heating power required to maintain battery safety. The heating power in the external heating method is limited by the risk of local over-heating, in particular for thick cells. As a result, the external heating method is restricted to ~20 min slow heating for a 30 °C temperature rise. In contrast, the SHLB is demonstrated to reach a heating speed of 1–2 °C/sec, ~40 times faster for large-size thick cells, with nearly 100% heating efficiency and spatially uniform heating free from safety concerns.

1. Introduction

Cost and reliability are major barriers to widespread adoption of electric vehicles (EVs) [1]. A viable approach to bring down EV cost and enhance reliability is to reduce the total cell count in a battery system by increasing the size of a single cell [2]. This saves space and weight occupied by inactive materials, and reduces the number of interconnectors and control circuits when integrated into a battery pack. The energy of a single automotive Li-ion cell has continued to increase over the years, from 0.012 kWh/cell of Tesla Model S (85 kWh pack, 7104 cells) and 0.125 kWh/cell of Nissan Leaf (24 kWh pack, 192 cells), to 0.208 kWh/cell of the upcoming 2017 Chev Bolt (60 kWh pack, 288 cells) and 0.348 kWh/cell of the 2017 BMW i3. Accordingly, the thickness of Li-ion single cells has increased to >35 mm, quadruple that of previous ones (e.g. the thickness of the 4-cell module in Nissan Leaf is 35 mm [3]).

Increasing the size or thickness of a single cell causes a great challenge to thermal management. The effective through-plane

* Corresponding author.
E-mail address: cxw31@psu.edu (C.-Y. Wang).

http://dx.doi.org/10.1016/j.jpowsour.2016.12.102
0378-7753/

thermal conductivity of Li-ion cells is rather low (<0.5 W $m^{-1}K^{-1}$) [4–6], mainly due to the high thermal contact resistance between individual cell components and low conductivity of separators. As cells become thicker, the poor through-plane heat transfer can result in large temperature non-uniformity across the cell, especially when there is large local heat source, such as in a battery heating process.

The performance of Li-ion batteries is notoriously poor at freezing temperatures [7–10]. The driving range of EV per charge, 105 miles at 23.9 °C as tested by American Automotive Association [11], drops by 57% to 43 miles at −6.7 °C. Fundamentally, poor battery performance at subzero temperatures is attributed to sluggish charge transfer kinetics, high electrolyte viscosity, and poor solid-state Li diffusivity. As these kinetic and transport processes depend highly upon temperature, cell performance recovers after warming up. Heating of batteries is hence vital for EV operation in cold environment [12–16]. In most EVs, heat comes only from two sources. The first one is powertrain waste heat from motor, inverters, and batteries. If the waste heat is insufficient, additional heat is produced via external resistive heaters. Hence, traditional battery heating in EVs can be divided into two strategies: internal heating via battery resistance, and external heating via resistors and circulated fluid.

One major issue of the conventional heating strategies is very slow heating speed, typically less than 1 °C/min. Batteries would stay at low performance and efficiency for a long time during EV operation in cold weather, wasting a great deal of battery energy. In addition, regenerative braking, accounting for ~20% of EV range in optimal conditions, cannot be performed when the battery temperature is low due to the risk of lithium plating [17]. Significantly increasing the heating speed, therefore, is of vital importance to beat the winter woes and ensure all-climate operability of EVs. Recently, Wang and co-workers [18] developed a novel battery structure, named self-heating Li-ion battery (SHLB), that can achieve rapid heating, i.e. >1 °C/sec, of Li-ion cells. In the present work, the conventional heating strategies are compared with the new SHLB structure to elucidate fundamental reasons for the huge leap in heating speed. Moreover, we illustrate the technical challenge of conventional heating strategies associated with increasing cell thickness, and we present herein a novel solution to achieve rapid and uniform heating of large-size Li-ion cells.

2. Battery internal heating vs SHLB

The heating speed can be estimated via the basic heat balance equation as:

$$mc_p\Delta T = P_{heat}\cdot\Delta t \quad (1)$$

where m, c_p and T are mass, thermal capacity and temperature of the battery; P_{heat} and t are heating power and time.

We first analyze the scenario of internal heating via battery resistance, taking Nissan Leaf as an example. It has a 24 kWh battery pack, with reported energy density of 157 $Wh/kg_{battery}$ [3] (i.e. the total mass of batteries is ~152.8 Kg). Assuming that the battery can last for 3 h per charge (i.e. discharge rate of C/3, or battery power of 8 kW) and the discharge efficiency is 90%, the waste heat generated is 0.89 kW. With Eq. (1) and assuming $c_p = 1000\ J\ kg^{-1}\ K^{-1}$, the speed of internal heating is ~0.0058 °C/sec, or 0.35 °C/min, which is 175× slower than the reported heating speed of SHLB (29.6-sec from −30 °C to 0 °C, ~1 °C/sec [18]).

To make a more direct comparison between SHLB [18] and internal heating of a conventional Li-ion cell, we assume that both cells discharge at the same current. The heating energy of the conventional cell can be estimated as $I \times (U_{ov}\text{-}V_{cell})$, with I, U_{ov} and V_{cell} denoting current, open-circuit voltage (OCV) and cell voltage. In SHLB, a thin nickel (Ni) foil is inserted into the cell. When heating is applied, current is directed to flow through the Ni foil. Hence, heat in SHLB comes from two sources: the cell and the Ni foil. Heating power of the cell is $I \times (U_{ov}\text{-}V_{cell})$, and of the foil is $I \times (V_{cell}\text{-}V_{act})$, with $V_{act} = 0$ V. The total heating energy of SHLB is thus $I \times U_{ov}$, indicating that all electrical energy of the battery is converted to heat in the heating process of SHLB (i.e. 100% heating efficiency). On the contrary, only a fraction of battery electrical energy is converted to heat during conventional internal heating. The ratio of heating energy between SHLB and conventional Li-ion cell with internal heating at the same current is hence $U_{ov}/(U_{ov}\text{-}V_{cell})$. Assuming $U_{ov} = 4.2V$, the heating energy of SHLB is 3.5× of the conventional cell at $V_{cell} = 3.0V$, and 21× at $V_{cell} = 4.0V$. In addition, it shall be noted that heating of conventional cells by intentionally discharging at high current is impractical in real EVs, as the output current of batteries depends on the power demand from the driver.

3. External heating of large-size cells

Another heating strategy in most of current EVs is external heating using resistive heaters placed on cell surfaces. For instance, Leaf uses 0.3 kW external heater, which can heat the battery only at ~0.1 °C/min according to Eq. (1). To accelerate heating, the power of external heater must be increased, which, however, may result in local overheating, especially for large-size thick cells, as will be discussed in this section. A prismatic cell structure is considered, as sketched in Fig. 1a, which is composed of multiple units of anode-separator-cathode assemblies. Two cell sizes are studied in this work. One is a 10 Ah cell used in our previous publications, which is chosen as a baseline case to represent the past or current generation of automotive Li-ion cells. The 10 Ah cell consists of 33 electrode-separator units, and the overall cell thickness is 9 mm. The second one is a 40 Ah cell composed of 132 units with cell thickness of 34 mm, similar to the thickness of the Samsung 94 Ah cell used in the new generation of BMW i3.

A 1-D thermal model is developed to resolve the temperature distribution across cell thickness, by solving the following heat conservation equation:

$$\frac{\partial(\rho c_p T)}{\partial t} = \nabla\cdot(\kappa\nabla T) \quad (2)$$

where ρ and κ are density and thermal conductivity. Following our previous work [19], the thickness, density, specific thermal capacity and thermal conductivity of each single cell unit is set as 253.9 μm, 1707.1 kg m^{-3}, 1195.2 J $kg^{-1}K^{-1}$ and 0.5 W $m^{-1}K^{-1}$ respectively. External heating is simulated by applying constant heat flux (i.e. constant heating power) at the two outer cell surfaces (left and right surfaces in Fig. 1a). For all cases studied, the cell is initially at −30 °C, and the heating process is completed when the minimal temperature inside the cell reaches 0 °C.

Fig. 2a and b plot the temperature distributions across the cell thickness at the end of heating with different heating power. The increase of heating power results in larger temperature gradient in the cell, with highest temperature at the surface and lowest in the center. Comparing Fig. 2a with 2b, it can be seen that the local temperature near the cell surface is much higher in the thick 40 Ah cell at the end of heating when the minimum temperature reaches 0 °C. Fig. 3a presents the variation of heating time with heating power for the two cells. The time of external heating is also compared with that of uniformly internal heating (UIH), which, theoretically, is the minimal heating time at a given power and can be calculated via Eq. (1). We can note that external heating takes much longer time than UIH at high heating power, mainly due to

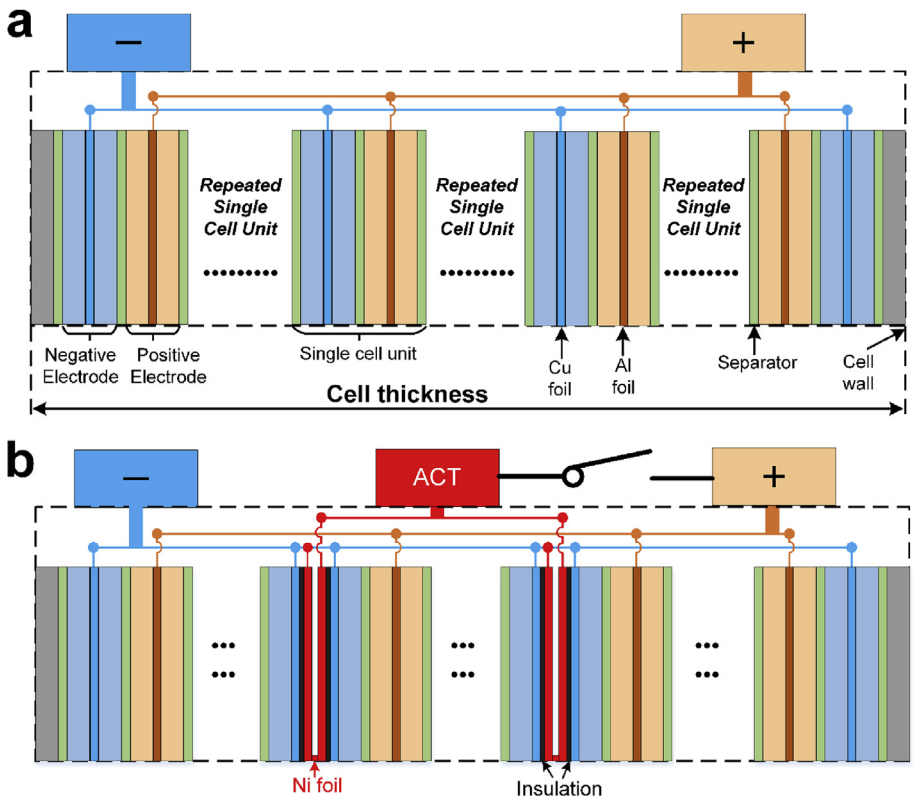

Fig. 1. Schematic illustration of (a) a conventional Li-ion cell and (b) a self-heating Li-ion battery with multiple Ni foils inserted.

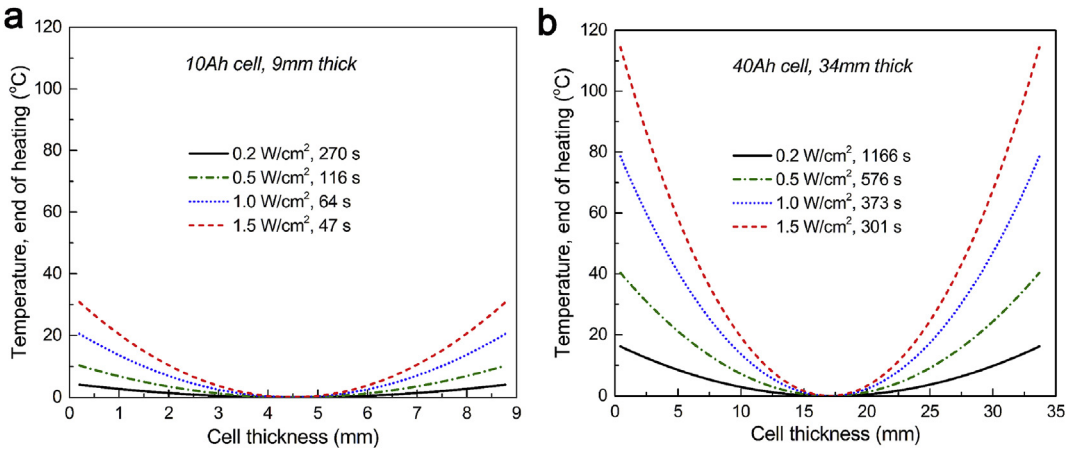

Fig. 2. Internal temperature distributions across cell thickness at the end of external heating (minimal internal temperature reaching 0 °C) with different heating power of (a) a 10 Ah cell and (b) a 40 Ah cell.

the temperature non-uniformity inside the cell. Also, the deviation in heating time between external heating and UIH is more dramatic for the thick 40 Ah cell and at higher heating power. The increase of cell thickness leads to much higher temperature near the cell surface, as can be seen from Fig. 3b. We shall note that the highest temperature inside the cell must be restricted (e.g. below 80 °C) for the sake of battery safety. As a consequence, the power of external heating has an upper limit.

Fig. 4a plots the maximum cell temperature against heating time with the data in Fig. 3a and b. From this plot, we can see a clear constraint between lowering maximum local temperature and reducing heating time (i.e. increasing heating power) in the case of external heating, and this constraint is more serious for the thick 40 Ah cell. For instance, if battery safety is a major concern and the maximum allowable temperature is set at 80 °C, the minimal time for external heating of the 10 Ah cell from −30 °C to 0 °C is 23.3 s at the maximal power of 4.56 W/cm^2. However, when the cell size increases to 40 Ah, the maximum allowable power of external heating drops to 1.02 W/cm^2, leading to the minimal heating time of 369 s. Fig. 4b plots the total heating energy normalized by the battery energy versus the heating time for both cells, where the heating energy consumption in percentage is indicative of energy deficiency, whereas the heating time is indicative of vehicle agility in winters. It is seen that reducing heating time always leads to

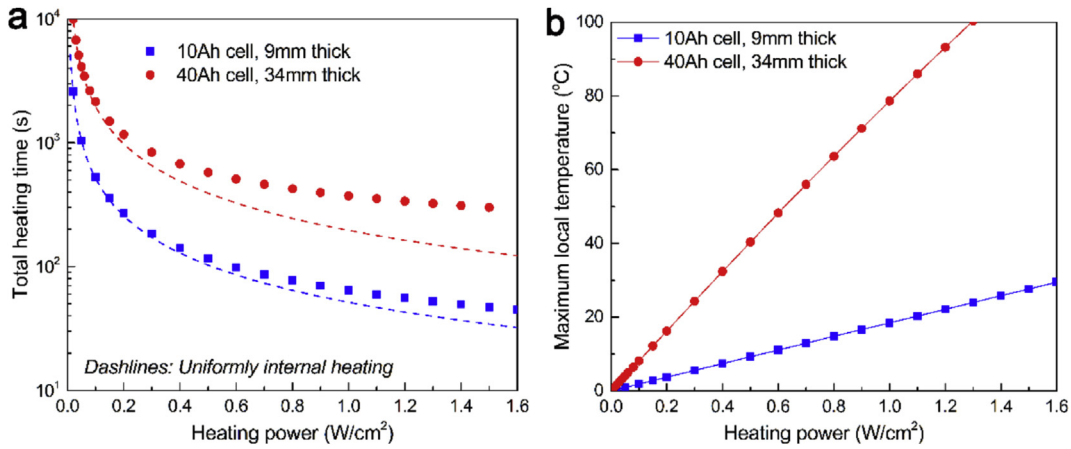

Fig. 3. Variation of (a) total heating time and (b) maximum local temperature with heating power for external heating of baseline and large-size cells.

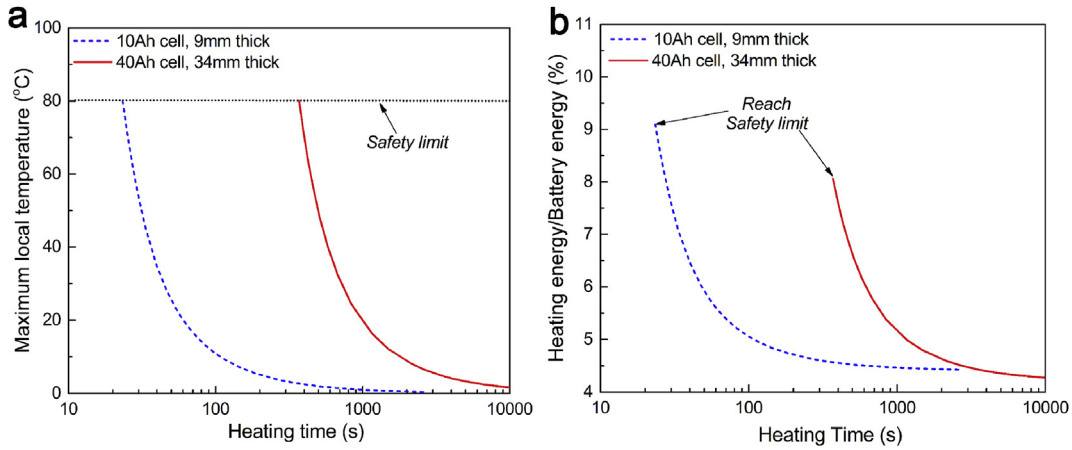

Fig. 4. Variation of (a) maximum local temperature and (b) ratio between total heating energy and battery energy with the total heating time for external heating of the baseline and large-size conventional Li-ion cells.

higher energy consumption in external heating. Moreover, the increase of cell size leads to much higher energy consumption at the same heating speed. For instance, at the maximum heating speed of the 40 Ah cell (heating power of 1.02 W/cm^2 and heating time of 369 s), the total heating energy accounts for 8% of the electrical energy contained in the 40 Ah cell. For the 10 Ah cell with the same heating time, the heating energy consumption is only 4.6% of the battery electrical energy.

4. Rapid and uniform heating of large-size SHLB cells

Based on the above discussion we can learn that it is vital to increase heating power while maintaining the temperature uniformity in order to reduce the heating time. From the analysis in Section 2 we note that the SHLB is advantageous in that it has 100% heating efficiency. Furthermore, the SHLB cell is also able to be heated uniformly, which can be particularly useful for large-size Li-ion cells, as will be presented in this section.

The structure of a SHLB pouch cell is sketched in Fig. 1b. Aside from components of a conventional Li-ion cell, the SHLB inserts one or several pieces of thin Ni foil, each coated with electrically insulating polymer and sandwiched between two single-sided anode layers. One end of the Ni sheets is welded together with anode tabs and connected to the negative terminal. The other end is welded together and extends outside the cell to form a third terminal, named the activation (ACT) terminal. A switch is added between the positive and ACT terminals. When heating is required, the switch is closed to force cell current to flow through the Ni foil to generate immense heat internally in the cell. Once cell temperature reaches a desired value, the switch is opened to terminate the heating process.

In previous work, we demonstrated that heating of SHLB can become more uniform with more Ni foils inserted [19,20], as it can shorten the path of heat transfer from heat generating foils to surrounding battery materials. This approach is used in this section for large-size cells. The SHLB cell studied here has the same size as the above 40 Ah conventional cell (132 single cell units). Four cell designs are investigated, with 3, 4, 6 or 8 pieces of Ni foil embedded. For all these designs, the overall resistance of the parallel-connected Ni foils is kept at 14 mΩ@20 °C, and the sum of Ni foil thickness is 200 μm. In other words, the resistance and thickness of each Ni foil are 42 mΩ and 66.67 μm in 3-sheet design, 56 mΩ and 50 μm in 4-sheet design, 84 mΩ and 33.33 μm in 6-sheet design, and 112 mΩ and 25 μm in 8-sheet design. The SHLB overall thickness is only 0.2 mm thicker than the above 40 Ah conventional cell, decreasing the volumetric energy density in Wh/L only by 0.58%. In addition, the added Ni foil weighs ~100 g per kWh battery with the cost of $1/kWh based upon Ni price of $10/kg [18]. Assuming a battery cost of $250/kWh, the added cost due to Ni foils is 0.4% of the baseline battery.

An electrochemical-thermal (ECT) coupled model developed in our previous work [19] is adopted here to simulate the heating and electrochemical behaviors of the above SHLB cells. A feature of this ECT model is that each single cell unit corresponds to an electrochemical model. In addition, a 1-D thermal model is solved along the cell thickness direction. As such, the ECT model is able to predict the current and temperature profiles across a multi-layer cell. Details about the ECT model can be found in Ref. [19]. Unless otherwise indicated, all model parameters in this paper are the same as in Ref. [19].

Fig. 5 shows the variation of cell current in the activation (heating) process of the four SHLB cells plus a control cell undergoing external heating. It can be seen that the current of all SHLB cells increase with time thanks to the decrease of cell internal resistance with rapid rise in temperature. The current of the external heating case, however, drops with time. Fig. 6 presents the evolution of internal temperature distribution with time in the case of external heating. Large temperature gradient builds up in the cell immediately upon heating. After only 15.8 s, the surface temperature reaches 80 °C, i.e. the safety limit, whereas a large portion of the cell still is at −30 °C, which is why the current of this control case decreases with time as discharge proceeds. The external heating process is aborted once the safety limit is reached.

Comparing the four SHLB cells in Fig. 5, it can be seen that the increase of Ni sheets leads to higher activation current. The internal temperature distribution at the end of heating (i.e. the surface temperature reaching 0 °C) is plotted in Fig. 7a. The local temperature peaks appear where Ni sheets are inserted. It can be clearly noted that the temperature distribution becomes much more uniform and the maximum internal temperature is reduced with more Ni sheets inserted. Fig. 7b presents the evolution of heating source generated by Ni foils (ohmic heating) and by the cell (electrochemical processes) during the heating process. It can be noted that most heat is generated on Ni foils. Taking the 8-sheet SHLB cell as an example, the thermal energy generated by the cell drops from 3.82 W/cm^2 (51.6% of total heat generation) at the beginning of heating to 1.53 W/cm^2 (16.9%) at the end. On the contrary, the heat generated by Ni foils increases from 3.58 W/cm^2 (48.4%) at the beginning to 7.54 W/cm^2 (83.1%) at the end. As mentioned in Section 2, the heat generation rate by the cell is equal to $I \times (U_{ov}\text{-}V_{cell})$ and by the Ni foil is $I \times V_{cell}$. Similar to our previous work [19], the

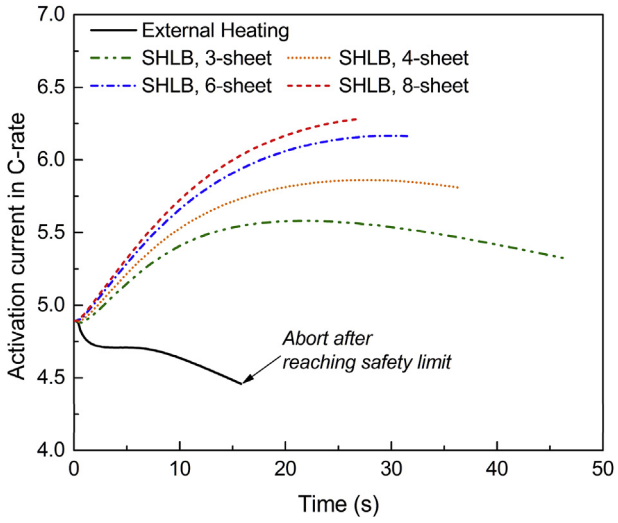

Fig. 5. Evolution of cell current in the heating process of self-heating Li-ion battery (SHLB) cells with different number of Ni sheets inserted and of the external heating case with Ni foils placed outside the cell.

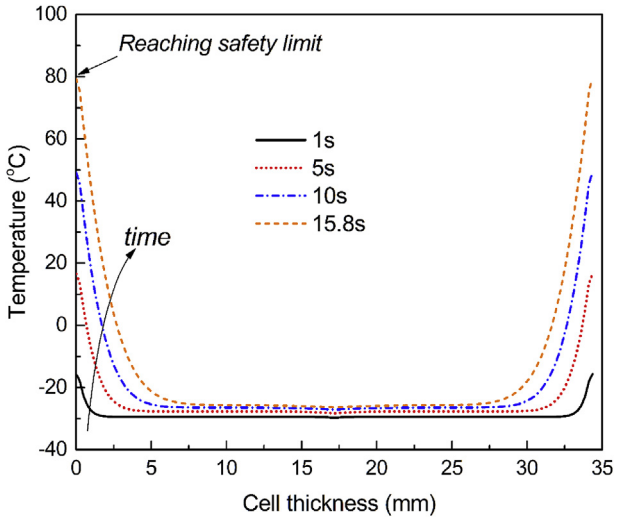

Fig. 6. Evolution of internal temperature distribution with time in the heating process of the controlled external heating case with Ni foils placed outside the cell from the ambient of −30 °C.

rise of cell voltage (V_{cell}) outpaces the increase of cell current in the activation process, thereby leading to the drop of heat generation by the cell and to the increase of heat generation on the Ni foils. Averaged over the entire heating process, heat generation by the cell and by the Ni foils are 2.67 W/cm^2 (31.4%) and 5.84 W/cm^2 (68.6%) respectively. Therefore, if there is no Ni foil inside the cell (i.e. internal heating of conventional Li-ion cells), the heating power (or heating speed) will be 3.2 times lower than the SHLB. In addition, we shall note that the overall heating power of 8-sheet SHLB cell is 8.51 W/cm^2, much higher than the maximum allowable power of external heating for the same 40 Ah cell (1.02 W/cm^2 as shown in Fig. 3b).

Fig. 8a displays the maximum internal temperatures of the four SHLB cells versus the total heating time and compares to the external heating case. It can be concluded that the SHLB is inherently superior to external heating as its heating power is not restricted by the safety concern; as such, the SHLB is able to be heated rapidly and uniformly, especially for the 8-sheet cell. Moreover, consider a practically useful case with a maximum allowable temperature non-uniformity of 10 °C in order to avoid local state-of-charge (SOC) imbalance. It is clear from Fig. 8a that the minimal heating time achievable with external heating and SHLB becomes 1598 s and 26.8 s, respectively, for the 40 Ah cell. Here lies a clear value of the innovative solution offered by SHLB.

Fig. 8b further plots the total heating energy non-dimensionalized by the battery energy against the heating time for the four SHLB cells of 40 Ah along with the external heating case. While all previous discussions have assumed perfect thermal insulation of batteries for fundamental elucidation, here we also add a practical thermal insulation condition relevant to real EVs, i.e. the heat dissipation coefficient $h = 5\ W/m^2K$. A theoretical limit for the heating energy consumption in percent of battery energy can be easily determined by $c_p\Delta T$ divided by the gravimetric energy density of a cell, because the former simply represents the mass specific sensible heat needed to raise a temperature difference ΔT. Using the parameters of the 40 Ah cell, this lowest limit in heating energy consumption is also indicated in Fig. 8b. Although the two cases with different thermal boundary conditions have no dramatic difference in the maximum local temperature as shown in Fig. 8a, it is clearly seen from Fig. 8b that in the case of external heating with imperfect thermal insulation, the heating energy consumption

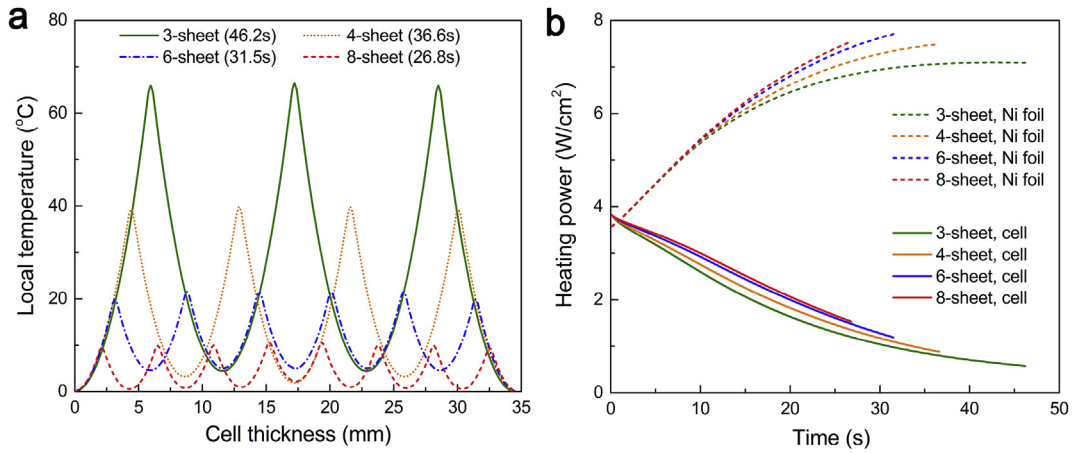

Fig. 7. (a) Internal temperature distribution across cell thickness at the end of heating (the surface temperature reaching 0 °C) of self-heating Li-ion battery (SHLB) cells with different number of Ni foils inserted. (b) Evolution of heat source generated by Ni foils and by the cell in the heating process of different SHLB cells.

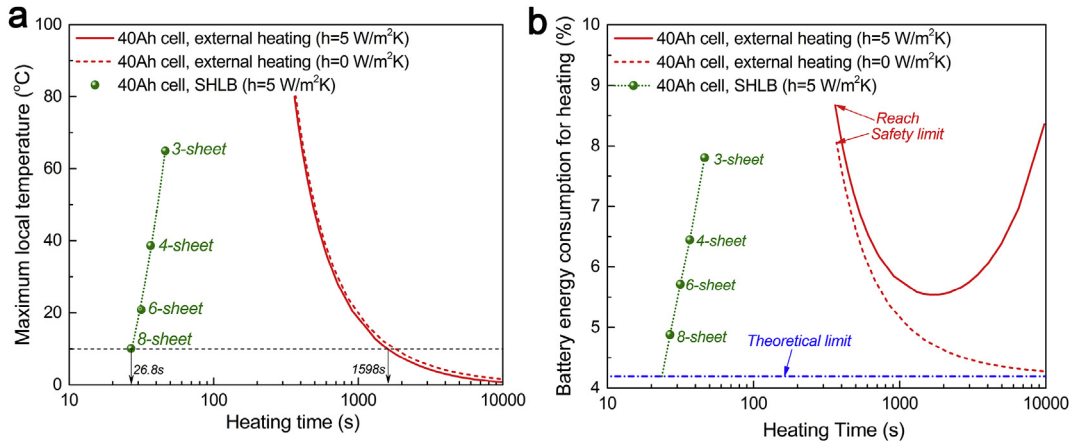

Fig. 8. Variation of (a) maximum local temperature and (b) ratio between total heating energy and battery energy with heating time for self-heating Li-ion battery (SHLB) cells with multiple Ni sheets inserted and conventional cells with external heating.

reaches a minimum as the heating time is extended but then rises again if the heating time is too great due to substantial heat loss over long period of time. On the other hand, the SHLB cells are insensitive to imperfect thermal insulation condition as the total heating time is kept so short. Overall, only the innovative solution of SHLB lies in the lower left corner of Fig. 8b where superior energy efficiency and high agility in battery heating can be made possible simultaneously.

5. Conclusion

Conventional Li-ion cell heating strategies, including internal heating via battery's resistance and external heating using resistive heaters, are compared with the recently proposed SHLB structure in this work, with particular focus on analyzing the huge leap in heating speed provided by SHLB over conventional Li-ion cells. Both internal heating and external heating of conventional Li-ion cells are slow because of their low heating power. The effectiveness of internal heating is largely limited by its low electrical-to-thermal conversion efficiency (i.e. roughly equal to the ratio of cell voltage to open circuit potential). For external heating, it is revealed that the increase of heating power is impeded by the risk of local overheating, in particular for thick cells. On the other hand, the SHLB is demonstrated to be an ideal choice for battery heating, especially for large-size thick cells. It achieves nearly 100% heating efficiency and ~40 times shorter heating time than presently used heating methods, and can be heated uniformly with the aid of multiple Ni foils embedded inside the cell. This new paradigm in battery heating thus makes electric cars highly agile and energy-efficient even in cold climates, opening a new era of weather-independent, robust EVs.

Acknowledgements

Partial financial support by Pennsylvania Department of Environmental Protection is gratefully acknowledged. We also thank EC Power for donation of AutoLion™ software for electrochemical-thermal coupled simulations presented in this work.

References

[1] D.L. Wood Iii, J. Li, C. Daniel, J. Power Sources 275 (2015) 234–242.
[2] K.J. Lee, K. Smith, A. Pesaran, G.-H. Kim, J. Power Sources 241 (2013) 20–32.
[3] http://www.eco-aesc-lb.com/en/product/liion_ev/.
[4] J. Zhang, B. Wu, Z. Li, J. Huang, J. Power Sources 259 (2014) 106–116.
[5] Y. Ye, L.H. Saw, Y. Shi, K. Somasundaram, A.A.O. Tay, Electrochim. Acta 134 (2014) 327–337.
[6] V. Vishwakarma, C. Waghela, Z. Wei, R. Prasher, S.C. Nagpure, J. Li, F. Liu, C. Daniel, A. Jain, J. Power Sources 300 (2015) 123–131.
[7] H.P. Lin, D. Chua, M. Salomon, H.C. Shiao, M. Hendrickson, E. Plichta, S. Slane, Electrochem. Solid State Lett. 4 (2001) A71–A73.

[8] S.S. Zhang, K. Xu, T.R. Jow, Electrochim. Acta 48 (2002) 241–246.
[9] S.S. Zhang, K. Xu, T.R. Jow, J. Power Sources 115 (2003) 137–140.
[10] Y. Ji, Y.C. Zhang, C.Y. Wang, J. Electrochem. Soc. 160 (2013) A636–A649.
[11] Extreme Temperatures Affect Electric Vehicle Driving Range, AAA Says, http://newsroom.aaa.com/2014/03/extreme-temperatures-affect-electric-vehicle-driving-range-aaa-says/.
[12] A. Vlahinos, A.A. Pesaran, Energy Efficient Battery Heating in Cold Climates, SAE Technical Paper, 2002. No.2002-01-1975.
[13] T.A. Stuart, A. Hande, J. Power Sources 129 (2004) 368–378.
[14] Y. Ji, C.Y. Wang, Electrochim. Acta 107 (2013) 664–674.
[15] J. Zhang, H. Ge, Z. Li, Z. Ding, J. Power Sources 273 (2015) 1030–1037.
[16] H. Ruan, J. Jiang, B. Sun, W. Zhang, W. Gao, L.Y. Wang, Z. Ma, Appl. Energy 177 (2016) 771–782.
[17] Z. Li, J. Huang, B. Yann Liaw, V. Metzler, J. Zhang, J. Power Sources 254 (2014) 168–182.
[18] C.Y. Wang, G. Zhang, S. Ge, T. Xu, Y. Ji, X.G. Yang, Y. Leng, Nature 529 (2016) 515–518.
[19] X.G. Yang, G. Zhang, C.Y. Wang, J. Power Sources 328 (2016) 203–211.
[20] G. Zhang, S. Ge, T. Xu, X.G. Yang, H. Tian, C.Y. Wang, Electrochim. Acta 218 (2016) 149–155.